Hindawi
Geofluids
Volume 2021, Article ID 1268352, 6 pages
https://doi.org/10.1155/2021/1268352

Research Article

Investigation of Fracture Width Change under Closure Pressure in Unconventional Reservoir Based on the Hertz Contact Theory

Lifei Dong,[1,2,3] **Di Wang**,[1,2,4] **Fengxia Li**,[1,2,4] **Xinye Fu**,[5] **and Miao Wang**[6]

[1]*State Key Laboratory of Shale Oil and Gas Enrichment Mechanisms and Effective Development, Beijing 100083, China*
[2]*National Energy Shale Oil Research and Development Center, Beijing 100083, China*
[3]*College of Civil Engineering, Chongqing Three Gorges University, Chongqing 404120, China*
[4]*SINOPEC Petroleum Exploration and Production Research Institute, Beijing 100083, China*
[5]*College of Civil Engineering, Chongqing University, Chongqing 400044, China*
[6]*College of Mathematics and Statistics, Chongqing Three Gorges University, Chongqing 404120, China*

Correspondence should be addressed to Lifei Dong; lfdong2012@sina.com

Received 22 July 2021; Accepted 19 August 2021; Published 13 September 2021

Academic Editor: Feng Yang

To describe the fracture width is crucial for the flow conductivity evaluation, which influences the exploitation efficiency of unconventional oil and gas resources. Commonly, as the proppants fill in the fracture, the deformation will happen under the closure pressure to resist the fracture width change. Therefore, it is significant to develop the theoretical model to predict the variation. In this work, the mathematical model for the propping behavior of proppants in the fracture under closure pressure is established based on the Hertz contact theory. Compared with the existing models, the developed model considers both the proppant insertion and the elastic compression among the proppants, which is closer to the actual physical process. Furthermore, the experimental cases with different proppant sizes are taken to verify the model, and the good conformity presents its rationality. The parameter sensitivity analysis of this model shows that the fracture width change increases with the increase of the average diameters of proppants (D) and it declines with the improving of proppant elasticity modulus (E_1) and Poisson's ratio (ν_1).

1. Introduction

The hydrofracture technology is common during the development of unconventional oil and gas reservoirs [1–4]. The fracture net there will be formed after the hydrofracture process to provide the seepage channel of fluids, composed by the natural fracture and the induced fracture [5–9]. The proppants will be transferred into the facture during this stage [10, 11]. After soaking in the reservoir for a time, the production follows from the same interval of the hydrofracture. Once the production starts, the pore pressure will decline obviously, and the fracture width will decrease. As the proppants partly remain in the fracture, the propping effect is motivated to keep the fracture open, which is expected [12–15]. The competition between the proppants and the closure pressure influences the fracture width and the flow conductivity there, which relates to the development efficiency [16–18]. Thus, it is of great significance to study the antipressure ability of proppants and to describe the fracture width change under closure pressure.

Physically, the proppants in the fracture will be compressed or embedded during the antipressure process that leads to the change of fracture width. The relationship between the embedded degree of proppants and the closure pressure, proppant concentration, and mechanical properties of rock was studied early in 1998 by experiments [19]. Further, Guo and Zhang tested the influence of the proppant types, proppant size, and its paved concentration to the embedded degree in the fracture [20]. Li developed the flow conductivity test instrument and investigated the mineral

composition and mechanical parameter of the tight oil reservoir and reported the significant effect of brittle minerals and argillaceous material on insertion [21]. Innovatively, the backtracking method of proppants with nonradioactive elements was used to estimate the fracture width by well logging. However, this method requires high-quality well cementation, which limited its application [22]. Furthermore, the conditions of high temperature and high pressure were considered to analyze the influence of the fracturing fluid on the fracture width and its flow conductivity [23].

For the theoretical researches, the mathematical model for the proppants' inserted value under the closure pressure was established by microelement analysis, and the sensitivity analyses of the proppant size and the Young modulus of rock were discussed [24–26]. Zhao et al. derived the proppant insert depth model by using the elastic theory and also did the sensitivity analysis of basic parameters [27]. The numerical method was taken to present the fracture flow conductivity affected by the size and the layer number of proppants [13, 28–30].

Although these studies discussed the insertion process of proppants and the influence factors of flow conductivity, they were mostly based on the assumption of a stiff ball and ignore the deformation among the proppants. So the change of fracture width under closure pressure could not be described accurately. Specifically, the theoretical model considering the elastic mechanics of proppants needs to be developed.

In this paper, the theoretical model of fracture width change under the closure pressure, considering the elastic deformation among the proppants, will be established. Then, the experimental cases will be provided to verify the rationality of this model. And finally, the parameter sensitivity, such as proppant size, elasticity modulus, and Poisson's ratio, will be discussed.

2. Theoretical Model

In this section, a novel propped fracture width model for proppants compressed in the fracture under closure pressures is presented. In this work, the Hertz contact theory is used to establish the forces relationship effectively.

2.1. Model Assumptions. The proppants in the fracture are compressed, which cause the decrease of the fracture width. In order to describe the deformation under the closure pressure, some assumptions are put forward as follows:

(1) The proppants in the fracture are assumed to be spherical with the radius of "R_1." The proppants are distributed by connecting with each other (Figure 1). And the compaction of proppants due to the closure pressures is treated as a grain elastic deformation in this paper, which fits for the Hertz contact theory.

(2) The material properties of proppants keep stable during the deformation process. The compaction is contributed from two parts, the fracture wall layers (proppants A in Figure 1(c)) and the interlayers (proppants B in Figure 1(c)). The stable shape of proppants is modeled as the hexagon after compression (seen in Figure 1).

(3) Under the action of fracture closing, proppants will be compressed and deformed. The forces affecting the compressed proppants are in equilibrium. The closure pressure "P_c" affects the fracture walls, which is equal to the difference between the overburden pressure "P_o" and the pore pressure "P_p." The compressed force among proppants "N" keeps balance with the closure pressure "P_c." The gravity and buoyancy on the proppants are ignored in the fracture during the compaction.

2.2. Fracture Width Change Modeling

2.2.1. The Proppant Insertion Is Not Considered. For the layer A, the proppants make contact with the fracture wall directly. According to the Hertz contact theory [31–33], the normal force can be expressed as follows:

$$N = \frac{4}{3}\frac{E_1E_2}{E_2\left(1-\nu_1^2\right)+E_1\left(1-\nu_2^2\right)}\left(\frac{R_1R_2}{R_1+R_2}\right)^{1/2}{\alpha_1}^{3/2}, \quad (1)$$

where "R_1" and "R_2" are the radii of the proppant and the fracture wall, respectively; "E_1" and "E_2" are the elasticity moduli of the proppant and the fracture wall, respectively; "ν_1" and "ν_2" are Poisson's ratios of the proppant and the fracture wall, respectively; and "α_1" is the compaction value.

As the conditions, $R_2 \longrightarrow \infty$, $E_2 \gg E_1$, Equation (1) can be simplified as

$$N = \frac{4}{3}\left(\frac{E_1}{1-\nu_1^2}\right){R_1}^{1/2}{\alpha_1}^{3/2}. \quad (2)$$

Based on research [34], the normal force "N" can also be expressed as

$$F = 2\sqrt{3}P_cD^2 = 8\sqrt{3}P_c{R_1}^2, \quad (3)$$

where "F" is the compress force on the proppants, "P_c" is the fracture closure pressure, and "D" is the diameter of proppants.

For the proppants A, the compress force "F" is equal to the normal force:

$$F = N. \quad (4)$$

According to the force analysis, the fracture closure pressure "P_c" is equal to

$$P_c = P_o - P_p, \quad (5)$$

where the "P_o" is the overburden pressure and "P_p" is the pore pressure.

Combining Equations (2), (3), (4), and (5), the compaction value "α_1" can be expressed as

$$\alpha_1 = \left[6\sqrt{3}\left(P_o - P_p\right)\left(\frac{1-\nu_1^2}{E_1}\right)\right]^{2/3}R_1. \quad (6)$$

The number of proppant layers contacting with the fracture walls is 2 (the top layer and the bottom layer), so the

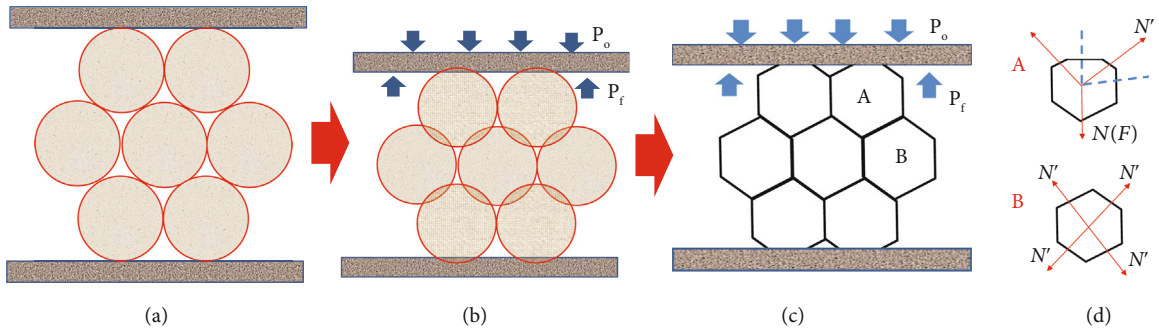

Figure 1: Compression model of proppants in fracture under closure pressures: (a) proppant heap without compaction; (b) proppant deformation under compaction; (c) model of compressed proppants; (d) force analysis for different proppants.

compaction caused by the proppants A is

$$h_1 = 2\alpha_1 = 9.532\left[\left(P_o - P_p\right)\left(\frac{1-\nu_1^2}{E_1}\right)\right]^{2/3} R_1. \quad (7)$$

For the layer B, the proppants are in contact with the other proppants. So the conditions are, $R_2 = R_1$, $E_2 = E_1$, and $\nu_2 = \nu_1$. And the normal force can be expressed as follows:

$$N' = \frac{2}{3}\frac{E_1}{\left(1-\nu_1^2\right)}\left(\frac{R_1}{2}\right)^{1/2}\alpha_2^{3/2}. \quad (8)$$

According to the force analysis in Figure 1(d),

$$N' = \frac{2F}{\sqrt{3}}. \quad (9)$$

Combining Equations (3), (8), and (9), the compaction value "α_2" can be expressed as

$$\alpha_2 = \left[24\sqrt{2}P_c\left(\frac{1-\nu_1^2}{E_1}\right)\right]^{2/3} R_1. \quad (10)$$

If the number of proppant layers is "n," the compaction value for this part is

$$h_2 = (n-1)\alpha_2 = 10.494(n-1)\left[\left(P_o - P_p\right)\left(\frac{1-\nu_1^2}{E_1}\right)\right]^{2/3} R_1. \quad (11)$$

So the total compaction degree can be established as

$$h = h_1 + h_2 = [9.532 + 10.494(n-1)]\left[\left(P_o - P_p\right)\left(\frac{1-\nu_1^2}{E_1}\right)\right]^{2/3} R_1. \quad (12)$$

2.2.2. The Proppant Insertion Is Considered. If the insertion for the proppants is considered, the conditions turn to $R_2 \longrightarrow \infty$ and Equation (1) can be simplified as

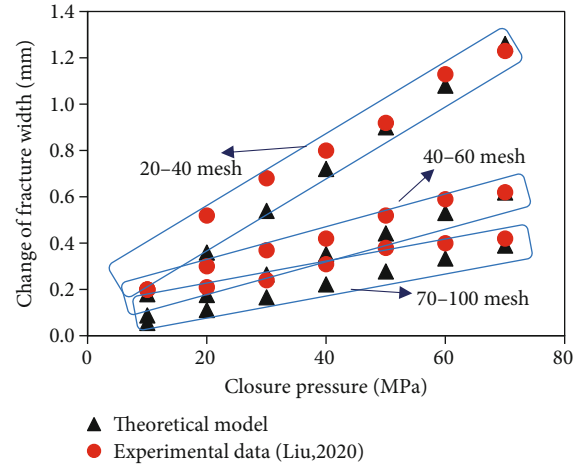

Figure 2: Experimental data of Liu [35] versus predicted results from our derived model in Equation (15) with different closure pressure conditions.

$$N = \frac{4}{3}\frac{E_1E_2}{E_2\left(1-\nu_1^2\right)+E_1\left(1-\nu_2^2\right)}R_1^{1/2}\alpha_1^{3/2}. \quad (13)$$

The compaction between the proppant A and the fracture wall should be adjusted as

$$\alpha_1 = \left[6\sqrt{3}\left(P_o - P_p\right)\left(\frac{1-\nu_1^2}{E_1}+\frac{1-\nu_2^2}{E_2}\right)\right]^{2/3} R_1. \quad (14)$$

The compaction value for the proppant B part is the same. And the total compaction degree is

$$\begin{aligned} h &= 2\alpha_1 + (n-1)\alpha_2 \\ &= \left[9.532\left(\frac{1-\nu_1^2}{E_1}+\frac{1-\nu_2^2}{E_2}\right)^{2/3} + 10.494(n-1)\left(\frac{1-\nu_1^2}{E_1}\right)^{2/3}\right] \\ &\quad \cdot \left(P_o - P_p\right)^{2/3} R_1. \end{aligned} \quad (15)$$

3. Results and Discussion

3.1. Model Verification. To invest the influence factors of hydraulic propped fracture conductivity in shale reservoir,

Table 1: Deviation between the experimental data and the theoretical model.

Mesh	Deviation ratio (%)						
	10 MPa	20 MPa	30 MPa	40 MPa	50 MPa	60 MPa	70 MPa
20-40	66.62	1.75	1.97	5.01	5.97	2.57	0.79
40-60	18.20	13.42	8.00	1.81	7.96	8.39	3.38
70-100	48.50	22.12	10.69	16.24	20.70	14.92	10.20

Liu [35] took the proppant type, particle size, sand concentration, cyclic stress, and fracturing fluid backflow into consideration, and the laboratory experiments on the effects of these factors were carried out. The proppants with the sizes of 20-40 mesh, 40-60 mesh, and 70-100 mesh were used, and the changes of fracture width under the closure pressure were discussed in research [35].

Figure 2 compares the experimental data of fracture width change under the closure pressure with different proppant sizes from Liu [35] and our predictions from Equation (15). The type of proppants is ceramsite proppants, which has the elasticity modulus "E_1" and the Poisson's ratio "ν_1" of 11306 MPa and 0.2, respectively. The average proppant diameters are 0.55 mm (20-40mesh), 0.27 mm (40-60mesh), and 0.17 mm (70-100mesh). What is more, the elasticity modulus "E_2" and the Poisson's ratio "ν_2" of the fracture matrix are 8000 MPa and 0.25, respectively. The closure pressure changes from 0 to 70 MPa.

It can be seen that, for different ceramsite proppant sizes, the change of fracture width under different closure pressures predicted from the derived model keeps consistent with the one from experimental data [35]. The deviation between the experimental data and the theoretical model is shown in Table 1. The deviation is relatively high in the low closure pressure, and it is because the contact is not sufficient, while the residual in the high closure pressure is very small. As a consequence, the proposed model in this paper is accurate, which conforms to the physical mechanism of proppants propping in the fracture, and benefits for the prediction of fracture width under the closure pressure condition.

3.2. Parameter Sensitivity Analysis. In this section, we will use this derived model for the sensitivity analysis of different conditions on the change of the fracture width under closure pressure.

Figure 3 shows the change of the fracture width versus the closure pressure with different parameter values D (the elasticity modulus "E_1" is 11306 MPa and the Poisson's ratio "ν_1" is 0.2). The results reveals that, for a given closure pressure, the fracture width change enlarges with the increase of average diameters of proppants D. The main reason is that a larger value of proppant diameters can cause more deformation. Moreover, as depicted in Figure 3, the curve of the fracture width change varies more severely for the higher value of D. So the larger diameter proppants have less compressed resistance, which is not expected.

Figure 4 shows the influence of different values of elasticity modulus E_1 on the fracture width change curve. The parameter values are given (the average proppant diameter

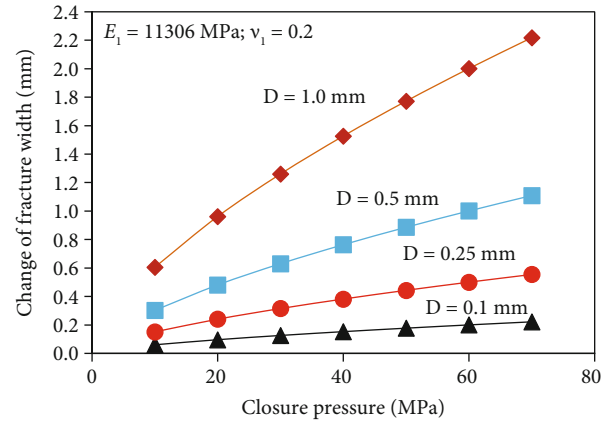

Figure 3: Fracture width change versus closure pressure with different parameter values D.

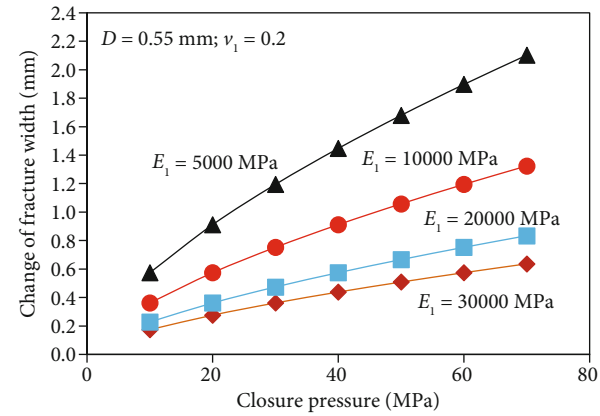

Figure 4: Fracture width change versus closure pressure with different parameter values E_1.

D is 0.55 mm and the Poisson's ratio ν_1 is 0.2). As we can see from the figure, under a specific closure pressure, the fracture width change decreases with the increase of the elasticity modulus E_1. The main reason is that the elasticity modulus E_1 has the negative relationship with the deformation degree. So a larger value of E_1 means more deformation of the fracture. Meanwhile, the curve varies more severely for the smaller value of E_1. So the proppants with the larger value of E_1 have more propping stability under different closure pressures.

Figure 5 presents the relationship between the fracture width change and closure pressure with different values of Poisson's ratio ν_1. Setting the value of basic parameter D as 0.55 mm, and the E_1 as 11306 MPa, the values of Poisson's

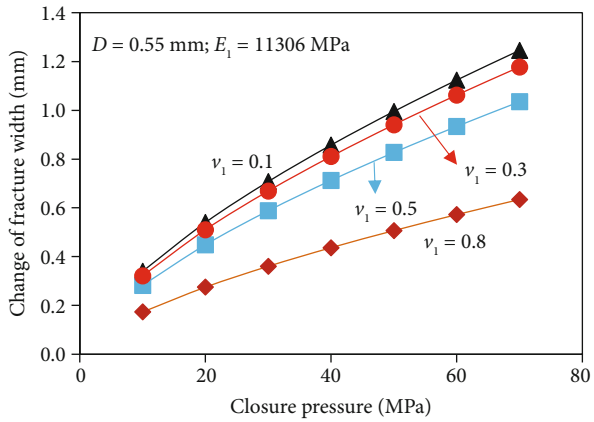

Figure 5: Fracture width change versus closure pressure with different parameter values ν_1.

ratio ν_1 change from 0.1 to 0.8. It can be seen that, under certain values of basic parameters, the change of fracture width has the negative relationship with Poisson's ratio ν_1, which means a lower Poisson's ratio ν_1 has the larger fracture width change under the closure pressure. And also, the curve for the lower value of Poisson's ratio ν_1 varies more seriously with the change of closure pressure.

3.3. Model Advantages and Limitations. The proposed model is established according to the actual physical background, which is the propping process for the proppants in the fracture under the closure pressure. It is common for the unconventional oil and gas exploitation. Besides, the model considers the different compressures between the boundary proppants and the interlayer proppants. With our derived model, the change of fracture width can be obtained, which can be used to explore the fracture conductivity further.

However, it should be also noted that the model has its limitations. The compressure process of proppants in the fracture, physically, can be divided into three stages with the increase of closure pressure, which are the elastic deformation stage, elastoplastic deformation stage, and fully plastic deformation stage. Our model focuses on the elastic deformation stage, which is the main factor for the fracture width change. However, the other two stages followed by the elastic deformation stage can also influence the proppants' deformation and fracture width. The corresponding works still need to be explored.

4. Conclusions

In this paper, a theoretical model is derived to predict the width change of the fracture, filled with proppants, under closure pressure by using the Hertz contact theory. It is verified by the experimental data of 3 different ceramsite proppant sizes, and the model result presents good consistency with the experimental finding. The proposed model considers the compressure of both the boundary proppants and the interlayer proppants under closure pressure, and the fracture width change is described conforming to the actual physical process.

The results of parameter sensitivity analysis in this model show that a positive relationship exists between the fracture width change and the closure pressure. Also, the basic parameters, such as the average diameters of proppants D, the elasticity modulus E_1, and the Poisson's ratio ν_1, influence the value of the fracture width change. For a given closure pressure, the change of the fracture width enlarges with the increase of D and declines with the improvement of E_1 (or ν_1). As the derived model mainly focuses on the elastic deformation of proppants and ignores the elastoplastic deformation and fully plastic deformation of proppants in the fracture under closure pressure, one should be cautious when using the model for analyzing the fracture conductivity.

Nomenclature

N: Normal force for Hertz contact (MPa)
R_1: Proppant radius (mm)
D: Proppant diameter (mm)
R_2: Radius of fracture boundary (mm)
E_1: Elasticity modulus of proppant (MPa)
E_2: Elasticity modulus of fracture wall (MPa)
ν_1: Poisson's ratio of proppant (dimensionless)
ν_2: Poisson's ratio of fracture wall (dimensionless)
α_1: Compaction value of boundary proppants (mm)
α_2: Compaction value of interlayer proppants (mm)
F: Compression force on the proppants (MPa)
P_c: Closure pressure (MPa)
P_o: Overburden pressure (MPa)
P_p: Pore pressure (MPa)
n: Number of proppants layer (dimensionless)
h: Fracture width change (mm)
h_1: Fracture width change contributed by boundary proppants (mm).

Data Availability

The [data type] data used to support the findings of this study are included within the article.

Conflicts of Interest

The authors declare that they have no conflicts of interest.

Acknowledgments

This work was supported by the Natural Science Foundation of Chongqing (cstc2019jcyj-msxmX0570), Scientific and Technological Research Program of the Chongqing Municipal Education Commission (KJQN201901216 and KJQN202001203), and Chongqing Engineering Research Center of Disaster Prevention & Control for Banks and Structures in Three Gorges Reservoir Area Program (SXAPGC21YB03).

References

[1] B. Deng, G. Yin, M. Li et al., "Feature of fractures induced by hydrofracturing treatment using water and L-CO_2 as fracturing fluids in laboratory experiments," *Fuel*, vol. 226, pp. 35–46, 2018.

[2] A. Medvedev, K. Yudina, M. K. Panga, C. C. Kraemer, and A. Peña, "On the mechanisms of channel fracturing," in *Paper SPE-163836-MS presented in SPE Hydraulic Fracturing Technology Conference*, Woodlands, Texas, USA, 2013.

[3] J. Wang, X. Zheng, Z. Wang, C. Tian, and C. Shi, "An approach to improve sweep efficiency of extra low permeability reservoir by vertical injector and producer with large scale hydrofracture," *SPE*, vol. 188047, 2017.

[4] F. Yang, B. Lyu, and S. Xu, "Water sorption and transport in shales: an experimental and simulation study," *Water Resources Research*, vol. 57, no. 2, 2021.

[5] K. S. Benjamin, "Cornucopia or curse? Reviewing the costs and benefits of shale gas hydraulic fracturing (fracking)," *Renewable and Sustainable Energy Reviews*, vol. 37, pp. 249–264, 2014.

[6] F. Yang, C. Xie, Z. Ning, and B. M. Krooss, "High-pressure methane sorption on dry and moisture-equilibrated shales," *Energy & Fuels*, vol. 31, no. 1, pp. 482–492, 2017.

[7] R. Zhang, B. Hou, P. Tan et al., "Hydraulic fracture propagation behavior and diversion characteristic in shale formation by temporary plugging fracturing," *Journal of Petroleum Science and Engineering*, vol. 190, article 107063, 2020.

[8] J. Zhang and S. Yin, "Some technologies of rock mechanics applications and hydraulic fracturing in shale oil, shale gas and coalbed methane," *Journal of China Coal Society*, vol. 39, no. 8, pp. 1691–1699, 2014.

[9] K. Zhang, N. Jia, S. Li, and L. Liu, "Static and dynamic behavior of CO_2 enhanced oil recovery in shale reservoirs: experimental nanofluidics and theoretical models with dual-scale nanopores," *Applied Energy*, vol. 255, p. 113752, 2019.

[10] X. Hu, K. Wu, G. Li, J. Tang, and Z. Shen, "Effect of proppant addition schedule on the proppant distribution in a straight fracture for slickwater treatment," *Journal of Petroleum Science and Engineering*, vol. 167, pp. 110–119, 2018.

[11] Y. Zou, X. Ma, and S. Zhang, "Numerical modeling of fracture propagation during temporary-plugging fracturing," *SPE Journal*, vol. 25, no. 3, pp. 1503–1522, 2020.

[12] C. Chen, V. Martysevich, P. O'Connell, D. Hu, and L. Matzar, "Temporal evolution of the geometrical and transport properties of a fracture/proppant system under increasing effective stress," *SPE Journal*, vol. 20, no. 3, pp. 527–535, 2015.

[13] K. Li, Y. Gao, Y. Lyu, and M. Wang, "New mathematical models for calculating proppant embedment and fracture conductivity," *SPE Journal*, vol. 20, no. 3, pp. 496–507, 2015.

[14] J. Wang and D. Elsworth, "Role of proppant distribution on the evolution of hydraulic fracture conductivity," *Journal of Petroleum Science and Engineering*, vol. 166, no. 1, pp. 249–262, 2018.

[15] X. Zheng, M. Chen, B. Hou et al., "Effect of proppant distribution pattern on fracture conductivity and permeability in channel fracturing," *Journal of Petroleum Science and Engineering*, vol. 149, pp. 98–106, 2017.

[16] Y. Lu, S. Han, J. Tang et al., "Experimental study of deformation and seepage characteristics of proppant under cyclic loading," *Rock and Soil Mechanics*, vol. 38, pp. 173–180, 2017.

[17] S. Man and R. Chik-Kwong Wong, "Compression and crushing behavior of ceramic proppants and sand under high stresses," *Journal of Petroleum Science and Engineering*, vol. 158, no. 9, pp. 268–283, 2017.

[18] W. Zheng, S. C. Silva, and D. D. Tannant, "Crushing characteristics of four different proppants and implications for fracture conductivity," *Journal of Natural Gas Science and Engineering*, vol. 53, no. 5, pp. 125–138, 2018.

[19] L. L. Lacy, A. R. Rickards, and D. M. Bilden, "Fracture width and embedment testing in soft reservoir sandstone," *SPE Drilling & Completion*, vol. 13, no. 1, pp. 25–29, 1998.

[20] T. Guo and S. Zhang, "Study on the factors affecting proppant embedment," *Fault-Block Oil and Gas Field*, vol. 18, no. 4, pp. 527–529, 2011.

[21] C. Li, Z. Zhao, J. Guo et al., "Experimental study on conductivity decline with proppant embedment in tight oil reservoir," *Petroleum Geology and Recovery Efficiency*, vol. 23, no. 4, pp. 122–126, 2016.

[22] J. Zhang, D. Harry, and J. Smith, "A determination of the capability of using gadolinium tagged proppant to evaluate propped fracture width," in *The Proceedings of SPWLA 58th Annual Logging Symposium. Houston: Society of Petrophysicists and Well Log Analysts*pp. 1–13, Oklahoma, USA, 2017.

[23] R. Matthew, Z. Ding, and D. H. Alfred, "Proppant fracture conductivity with high proppant loading and high closure stress," *SPE*, vol. 151972, 2012.

[24] Y. Li, Y. Liu, J. Jie et al., "Research on quantitative calculation model of proppant embedding in rock," *Journal of Southwest Petroleum University (Science & Technology Edition)*, vol. 33, no. 5, pp. 94–97, 2011.

[25] N. Cao and G. Lei, "Stress sensitivity of tight reservoirs during pressure loading and unloading process," *Petroleum Exploration and Development*, vol. 46, no. 1, pp. 138–144, 2019.

[26] W. Zheng and D. D. Tannant, "Grain breakage criteria for discrete element models of sand crushing under one-dimensional compression," *Computers and Geotechnics*, vol. 95, no. 3, pp. 231–239, 2018.

[27] J. Zhao, X. He, and Y. Li, "A calculation model of proppant embedment depth," *Joural of Oil and Gas Technology*, vol. 36, no. 12, pp. 209–212, 2014.

[28] B. N. Luiz, K. Aditya, and K. Andrei, "Conductivity and performance ofhydraulic fractures partially filled with compressible proppant packs," *International Journal of Rock mechanics & Mining Science*, vol. 74, no. 74, pp. 1–9, 2015.

[29] Y. Meng, Z. Li, and Z. Guo, "Calculation model of fracture conductivity in coal reservoir and its application," *Journal of China Coal Society*, vol. 39, no. 9, pp. 1852–1856, 2014.

[30] M. Chen, S. Zhang, M. Liu et al., "Calculation method of proppant embedment depth in hydraulic fracturing," *Petroleum Exploration and Development*, vol. 45, no. 1, pp. 159–166, 2018.

[31] L. Dong, X. Yue, Q. Su et al., "Study on the plugging ability of polymer gel particle for the profile control in reservoir," *Journal of Dispersion Science and Technology*, vol. 37, no. 1, pp. 34–40, 2016.

[32] Y. Li, L. Cheng, and W. Zhou, "A new prediction model of propped fracture width considering proppant deformation," *Science Technology and Engineering*, vol. 18, no. 6, pp. 107–113, 2018.

[33] J. Wu, M. Wang, and W. Wang, *An Introduction to Mechanics of Elasticity (Revised)*, Peking University Press, Beijing, 2001.

[34] W. Zhu, Q. Liu, M. Yue, and L. Zhang, "Calculation of frcature conductivity considering proppant influence and simulation of proppant transport in fracture," *Chemical Engineering of Oil & Gas*, vol. 48, no. 2, pp. 75–78, 2019.

[35] X. Liu, "Influencing factors of hydraulic propped fracture conductivity in shale reservoir," *Fault-Block Oil & Gas Field*, vol. 27, no. 3, pp. 394–398, 2020.